



A Photovoltaic Measurement System for Performance Evaluation and Faults Detection at the Field

Ahmed J. Abid^{1*} and Fawzi M. Al-Naima²

¹ Middle Technical University

² Fawzi M. Al-Naima

(Received 26 March 2019; Accepted 27 June 2019; Published on line 1 June 2020)

*Corresponding author: dr.ahmedjabbar@mtu.edu.iq

DOI: 10.5875/ausmt.v10i1.2144

Abstract: Testing and evaluation of the photovoltaic array are important issues for researchers and students alike in the renewable energy field. The collected data from the PV power plant gives a clear vision for the power plant production, array efficiency and fault detection. The presented system offers an electronic load connected to the PV array which is slightly increased from zero to the maximum designated value. It displays and stores all the voltage, current, and power measurements. It also calculates the voltage and current at the maximum power point, and the fill factor. All the measured data are documented within an Excel file on the computer; curves are plotted automatically to give the user a complete vision for the array behavior, power faults and the mismatching of the PV modules can be easily detected from these curves. The presented system describes all the electronic circuit schematics, how to select the appropriate electronic components with the proper rated values and offers a low-cost design that can be implemented with ease.

Keywords: Arduino Applications, Electronic load, Embedded system, Fault detection, PV array evaluation.

Introduction

The PV panel characteristics under real operating conditions which are determined using a fast-varying load [1], are usually different from those provided by the manufacturer under standard test conditions (25 °C, 1000W/m², AM=1.5) [2]. These conditions vary quickly and randomly according to many environmental factors [3], [4], so it is difficult to transcribe the physical characteristics of individual or array of PV panels. To overcome this problem, there is a need for a device that can test the PV system on site by loading it slightly from open circuit to short circuit conditions. Such a system has to be a fast-varying resistive load and capable of scanning the PV array curves with a dummy load in small varying steps to ensure gathering accurate results.

The existing commercial devices offer many such solutions for testing the PV arrays in the field, but they are expensive. Al Ameri, et al [5] presented an open loop system to control the load, but there is no feedback system to control the amount of current. Clustering the

array and tracking the behavior of each module over the power-line communication has also been presented as an alternative solution [6]. However, the proposed system is characterized by being a low cost and one that can be built with ease. It offers a precise voltage controlled current, and this technique can be used not only to study the PV array I-V curve characteristics, but also for tracking the maximum power point [7], control the PV battery charging current [8], testing power supply under high current [9], and detecting any fault in the PV array [10], [11].

Faults in PV array are mainly caused by mismatching effect [12]. This mismatching sometimes is irreversible error caused by mechanical or electrical problems, such as open circuit, short circuits and PV panel aging [13], or temporary power loss faults that are caused by sheltering [14] such as cloud shadows [15], and soiling accumulation [16]. All these faults have a specific influence on the PV array response, and many articles discussed how to recognize faults type from the PV array I-V and P-V curves [17], [18].

Such PV characteristics studying behavior and more are available on the presented system in this paper. It

increases the PV load slightly in small controlled and fixed steps. At each step the values of the PV voltage, current, and power are recorded and scanned to find the voltage and current at the maximum power point. Such data are important for monitoring the system health [17], or tracking the power at the maximum point [7].

The suggested circuit uses several N-channel Power MOSFET that are connected in parallel, as shown in Figure 1, according the application notes in [18], to handle the maximum load of the system. The driven current is completely controlled by a microcontroller. This microcontroller is used as a soft PID controller that measures the actual current and adjusts it to match the step planning current. This PID is very useful, since the MOSFET characteristics are temperature dependent. The article also presents a design for a dummy load based on a power MOSFET that can be connected to the PV array for testing in the field conditions. Such design is shown to be cost efficient, powerful, reliable, expandable, and easy to upgrade[19].

Photovoltaic Array in Brief

A typical equivalent circuit of a PV cell is shown in Figure 2a. In general, it consists of a main photocurrent source $I_{ph,cell}$ which is divided into three components; the diode current $I_{d,cell}$, the shunt resistor current $I_{p,cell}$,

and the main current I_{cell} . Figure 2b shows the equivalent circuit of an array of such PV cells. Normally, the PV module consists of PV cells connected in series to form a string to increase the module voltage. Finally, These PV modules may be connected in parallel, in series, or in a combination to make a PV array.

Table 1 displays the featured equations that describe these parameters when the PV cells are connected in an array [20]. The curves that describe the behavior of the current against voltage and power against voltage will be presented in the result and discussion section.

Power MOSFET Theoretical Analysis

Figure 3 shows the PV panel loaded by the drain resistance R_D of the linear Power MOSFET. When the operational amplifier balances the voltage on the inverting and the non-inverting inputs, the voltage V_G will be equal to the drop voltage, that is $I_D = V_G/R_S$ [19], [20]. The use of series resistance R_S has the following advantages:

- Linearize the voltage-controlled current response.
- Secure a feedback signal for the PID controller.
- Measure the supplied current by the PV array.
- Linearize the transconductance of individual MOSFETs in the parallel connection to avoid the current hogging.
- Share the load evenly between the paralleled MOSFET, even if they have different responses or characteristics. This can be accomplished by using two different techniques: (a) adjustable resistance, or (b) independent gate voltages, which makes it possible to drive each branch with different voltage.

Asst. Prof. Dr. Ahmed J. Abid received the B.Sc. and M.Sc. degrees in Electronic Engineering from the Department of Electrical and Electronic Engineering, University of Technology, Baghdad, Iraq in 2002 and 2004 respectively. He works as an academic visitor at Northumbria University, Newcastle upon Tyne, UK in 2013, then he received his Ph.D. degree in "Electronic and Communication Engineering" from University of Basrah, Basrah, Iraq in 2014. He has been working as an instructor in the Dept. of Electronic Engineering, Technical Instructor Training Institute (TITI), Middle Technical University, Baghdad, Iraq since 2006. He has been Head of the Technical Electronic Department at TITI (2014-2018), then assistant dean for scientific affairs and students.

Dr. Abid has published many scientific and technical papers in international and national journals and conferences. His research interests include solar photovoltaic farm, renewable energy, energy management, power line communication, embedded system design, internet of things, and fault detection in vast PV solar farms.

Email: dr.ahmedjabbar@mtu.edu.iq

Professor Emeritus Fawzi M Al-Naima received the degrees of BSc (First Class Honors), and PhD in Electrical Engineering from Newcastle University, UK in 1971 and 1976 respectively. He worked as a Lecturer and Associate Professor in Al-Rasheed College of Engineering, Baghdad, Iraq from 1977 to 1989. He joined the College of Engineering in Al-Nahrain University, Baghdad, Iraq as a Professor from 1989 to 2014. He served as a Dean of the College of Engineering from 2003 to 2007 in the same university. Professor Al-Naima has been serving as a Head of Department of Computer Engineering in Al-Mamoun University College, Baghdad- Iraq since October 2016.

Professor Al-Naima published more than 90 research papers in national and international journals and conferences. He is the co-author of a book on the analysis of large circuits published by an international publisher in USA, and the co-author of four chapters in four books published by international science publishers. Prof. Al-Naima current research interests include computer aided design of large circuits, analog and digital signal processing, solar tracking systems, and smart home energy managements. Professor Al-Naima is a Life Fellow Member of the IETE, India and a Senior Member of the IEEE.

Email: fawzi.alnaima@ieee.org

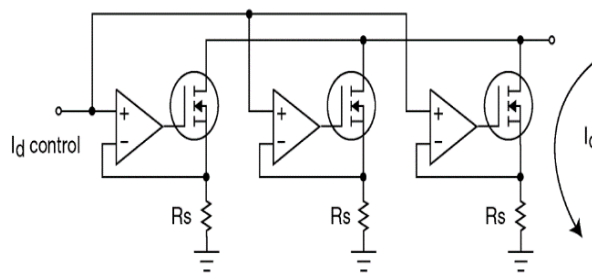


Fig. 1. Paralleling Several MOSFETs [18]

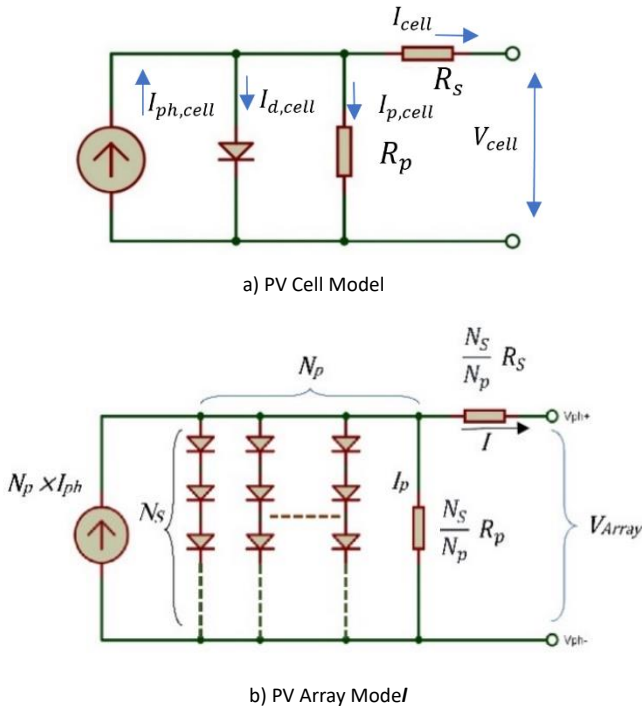


Fig. 3. Photovoltaic Equivalent Circuit

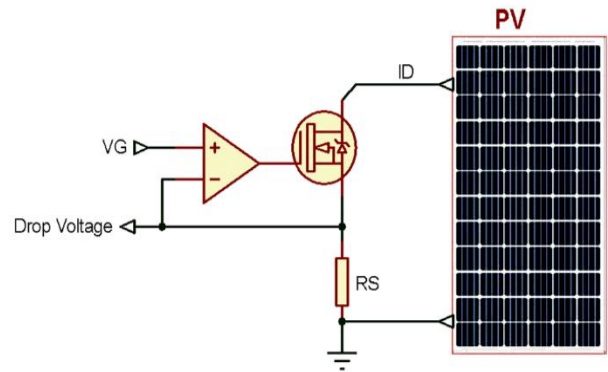


Fig. 2. MOSFET Driving Circuit

Table 1 PV Cell and PV Array Featured Equations

	PV Cell	PV Array
Main Current	$I_{cell} = I_{ph,cell} - I_{d,cell} - I_{p,cell}$	$I_{array} = I_{ph,array} - I_{d,array} - I_{p,array}$
Photocurrent	$I_{ph,cell} = \frac{G}{G_n} [I_{phn} + K_i(T_C - T_{ref})]$	$I_{ph,array} = N_p \times I_{ph,cell}$
Diode Current	$I_{d,cell} = I_{rs} \left\{ e^{\frac{(V+IR_s)}{V_T}} - 1 \right\}$	$I_{d,array} = N_p I_o \left\{ e^{\frac{1}{V_T} \left(\frac{V}{N_s} + \frac{IR_s}{N_p} \right)} - 1 \right\}$
Shunt Resistance Current	$I_{p,cell} = \frac{(V + IR_s)}{R_p}$	$I_{p,array} = \frac{N_p}{R_p} \left(\frac{V}{N_s} + \frac{IR_s}{N_p} \right)$
Shunt Resistance	$R_{p,cell}$	$R_{p,array} = \left(\frac{N_s}{N_p} \right) R_{p,cell}$
Series resistance	$R_{s,cell}$	$R_{s,array} = \left(\frac{N_s}{N_p} \right) R_{s,cell}$
Voltage	$V_{module} = (V_d - k_v \Delta T) - IR_s$	$V_{Array} = V_d N_s (1 - k_v \Delta T) - I \frac{R_s N_s}{N_p}$

Where V_d = diode voltage, N_s = number of cells in series, N_p = number of strings in parallel, T_c = Cell temperature in Kelvin, I_o = Diode reverse saturation current, R_s = Series resistance, R_p = parallel resistance, K_i = Current temperature coefficient, K_v = Voltage temperature coefficient, G_n = Standard solar Irradiance, G = Solar Irradiance, K = Boltzmann constant, V_T = Thermal Voltage (KTA/q), A = Ideality factor, I_{phn} = Photocurrent @STC, I_{rs} = Diode reverse saturation current, T_{ref} = The cell temperature at the standard test condition in Kelvin, and q = Electron charge.

SYSTEM DESIGN

In this section the system circuitry will be explained in a brief:

Current Control Circuit

This circuit is responsible for controlling and

measuring the driven current from the PV module. It consists of a number of sub-circuits, each having a specific duty as listed below with a brief description about their duties. The block diagram and the electronic design of this circuit are shown in Figure 4 and Figure 5 respectively. The descriptions of the sub circuits are as follows:

Low Pass Filter (LPF)

This circuit is used to convert the pulsed-modulated signal (PWM) from the microcontroller into smooth analog signal (0-5 V). It consists mainly of RC circuit (R1 and C1 as shown in Figure 5).

Analog Buffer

It is an operational amplifier (LM358N, U2:A in Figure 5) connected as buffer circuit. Its main duty is to buffer the LPF from the voltage divider and keep the LPF unaffected by the voltage driver and the next stages in the circuit.

Voltage Scaling

This circuit scales down the voltage to match the value of the sensing resistor. In this design the sensing current resistor is 0R1, so the voltage divider scales down the voltage by 90% of its original value. This sub circuit consists of R2 and R3 as shown in Figure 5.

Error Correction Driver

This circuit, which mainly consists of an operational amplifier (LM358N, U2: B in Figure 5), is responsible for controlling the voltage drop power MOSFET gate to keep the drop voltage at the sensing resistor equals to the driven voltage from the voltage divider.

Voltage Controlled Current

This is a Power N-Channel MOSFET IRFP460. According to its datasheet it can drive current up to 20 A (@ 20 °C), and its dissipation power is 280 W at 25 °C, hence it needs a heat sink and a fan to cool it down.

Sensing Resistor

This resistor R5 has two purposes; the first is to act as a feedback to balance the voltage-controlled current stage, and the second is to measure the actual delivered current by the PV module. This actual current will be used by the microcontroller to adjust the current into the set value.

Current Measurement Circuits

Since the value of the sensing resistor is too small, the accuracy of measured current will be low. For example,

if 1A current passes through the sensing resistor the drop voltage will be around 0.1 V and with microcontroller @ 5-volt reference voltage, the ADC accuracy will be very low (≈ 4.88 mV). Two options can be applied to improve the accuracy of the measured current. The first is by using a low reference voltage while the second is by amplifying the measured voltage. The system adopts an active LPF to smooth the measured signal and scale up the measured voltage as shown in 錯誤! 找不到參照來源。 . Resistors R6 and R7 are used for this purpose, according to the non-inverting amplifier gain equation ($A_v = 1 + R_6/R_7$).

Voltage Measurement Circuits

The adopted system is designed to measure a voltage in the range of (0-50 V), but with the Arduino ADC, the measured voltage is limited between 0-5V. So, it is required to step down the voltage from 50 V into 5 V and this can simply be achieved using a voltage divider circuit. Figure 5 shows the connection of the voltage divider circuit to the PV module. The measured voltage will be calculated according to the following expression: $V_{pv} \times R_{10}/(R_{10} + R_9)$; ie. if $R_{10} = 10$ k Ω , $R_9 = 90$ k Ω , the measured voltage will be ($V_{pv}/10$).

User Interface Devices

The system is completely interactive for the user, because it is mainly designed for training and testing purposes. Below is a list of these interactive devices:

Visual Interactive device

A GLCD (see Figure 6a), KS0108, 128×64 pixels, is used to display data and plot graphs.

Keypad device

A 4×4 matrix keypad (see Figure 6b) used to enter different types of data.

Set point circuit

This circuit (see Figure 6c) has a potentiometer to let the user enters the set point value. In the Auto Mode, the set point is considered as the current upper limit, but in the manual mode the user can use it to adjust the current directly.

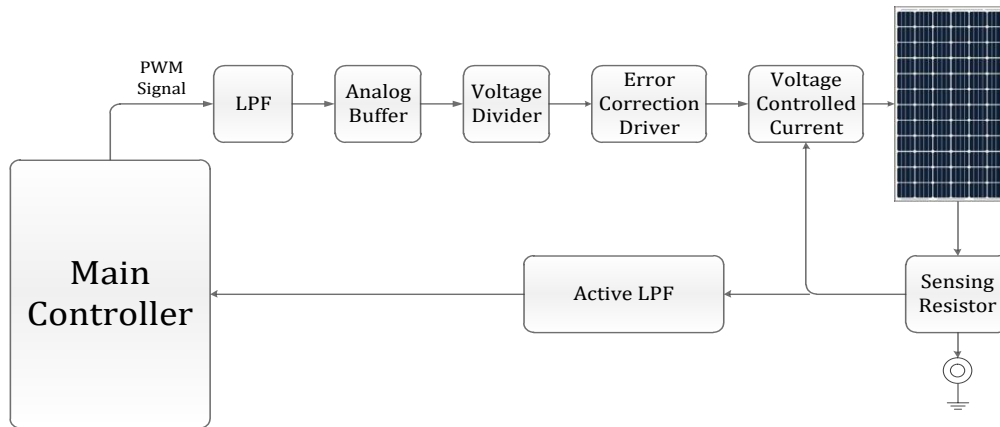


Fig. 4. Current Control Block Diagram

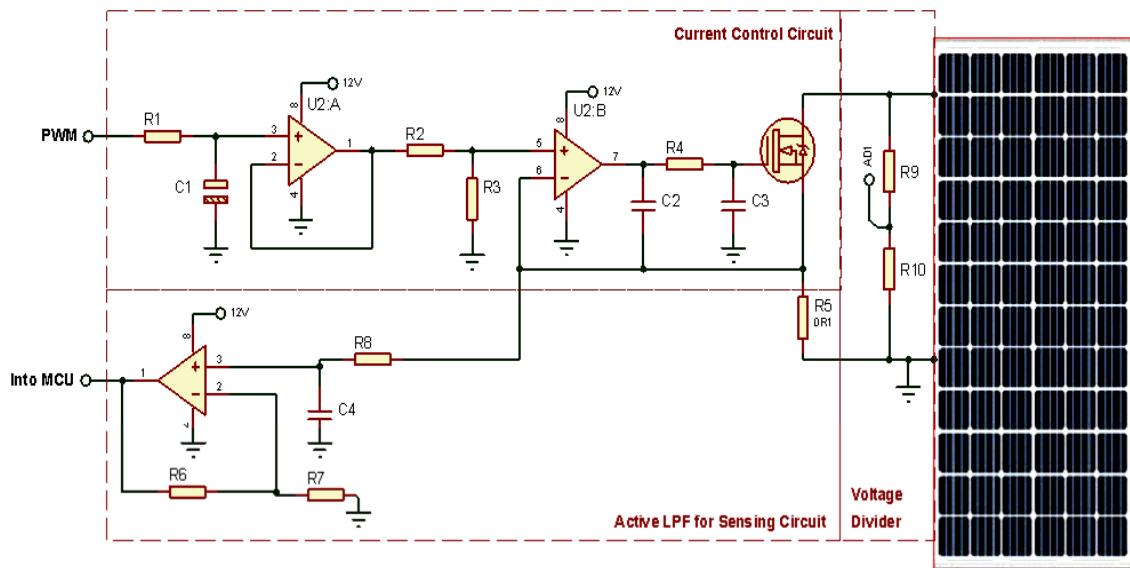


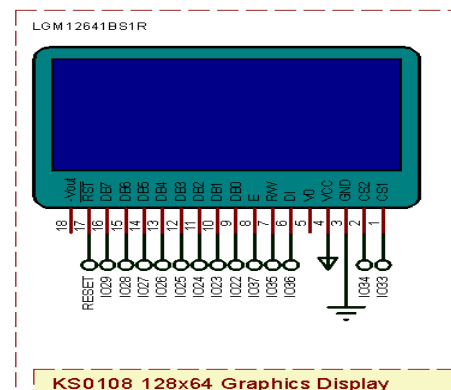
Fig. 5. Design of Current Controlled Circuit

Audio Interactive

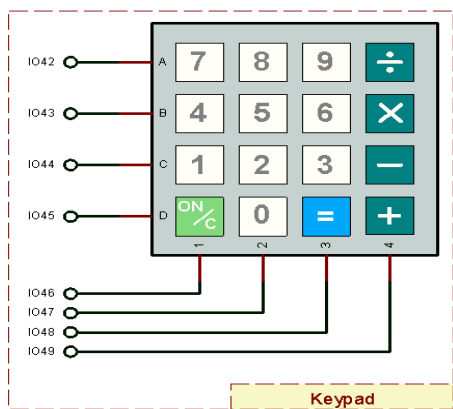
A buzzer used to warn the user with different sounds according to the warning types.

Serial Monitor

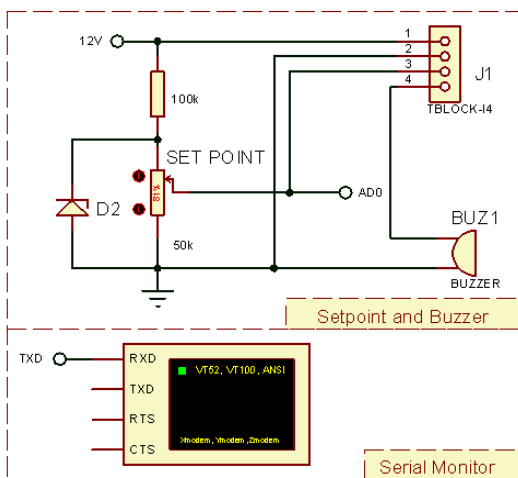
All the measured data are directly transmitted in the computer to be stored, monitored, and analyzed. It transmits the data at 115200 bps.



(a) GLCD



(b) Keypad



(c) Set point, Buzzer, and Serial monitor

Fig. 6. User Interface Devices

Load Management Strategy

The proposed system offers two modes of operation to manage the compensating load from the photovoltaic module; Auto Scanning Mode (ASM) and Manual Scanning Mode (MSM). In the ASM, the system will start to consume power from zero to zero watt, but in the MSM, it is fully controlled by the user. The flowchart in Figure 7 shows the adopted strategy for managing the system load. It starts by displaying Figure 8a, then it offers the two modes of operation and the user has to select one of them, see Figure 8b.

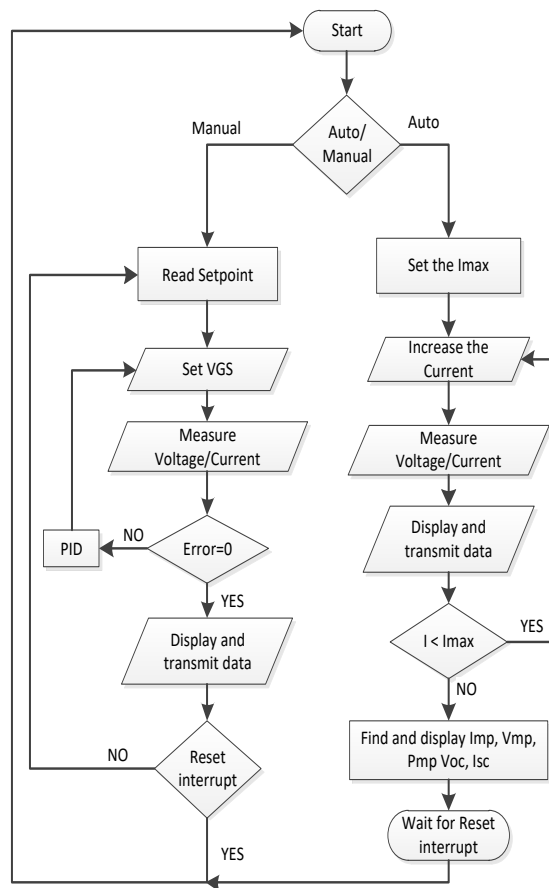


Fig. 7. The Load Management Strategy

Auto Scanning Mode (ASM):

An option will allow the system to inquire for any limitation imposed on the highest driven current from the PV panel as shown in Figure 8c. If this is not set, the system will increase the current until the voltage reaches 0V according to the PV characteristics. After this point, the system will start increasing the current until it reaches the maximum value, or the voltage reaches zero volt. The increment of the current will occur in small steps, ≈ 10 mA. In every step the system measures the actual system voltage, current, and power and displays them as depicted in Figure 8d. All these data will be transmitted to the computer. At the end of this scanning stage, the system obtains the open circuit voltage (VOC), short circuit current (ISC), voltage and current at the maximum power point (VMP, IMP), maximum power point (PMP), and the fill factor (FF) ($V_{mp}I_{mp}/V_{oc}I_{sc}$). These data will be displayed on the GLCD as shown in Figure 8e. Finally, the system will enter a freeze mode and wait for the user system reset, repeat the process, or select different modes.

Manual Scanning Mode (MSM):

In this mode the system reads the set point current periodically from the potentiometer. The accuracy of this current is an important matter, since the current must be

set exactly according to the set point no matter how much the voltage drops. To accomplish this, the system uses a PID controller to adjust the current. It increases or decreases the gate-source voltage VGS of the power MOSFET in time steps of 100 ms to match the set point. The used PID controller is a software library by the Arduino, it measures the output current and the set point and tries to keep the error approaching zero. The output voltage level is controlled via the duty cycle of the output PWM. The microcontroller displays and stores all these data into the computer by using the Arduino serial port and with the help of PLX-DAQ (Data Acquisition tool software add-in for Microsoft Excel acquires), see Fig. 8f. This mode stays active until it is interrupted by pressing the mode button on the keypad.

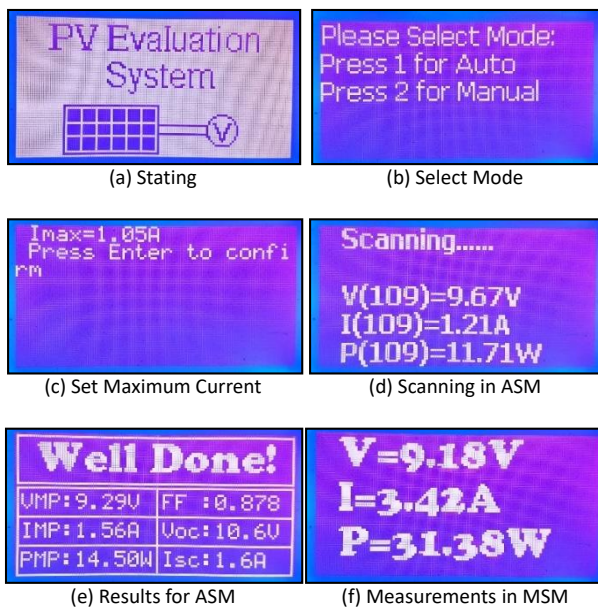


Fig. 8. Different Monitor Snapshots

SYSTEM IMPLEMENTATION

The heart of this system is the MOSFETs, as they are the main components that consume energy and the system has two of them, but more can be added as required. The used MOSFETs are N-Channel is having low RDON, (0.27 Ω), high current (20 A), and high voltage (500V). According to the data sheet such MOSFET can

dissipate up to 280 W @ 25 °C. A suitable aluminum heat sink with fan is attached to each MOSFET using a thermal adhesive. The current sensing resistor is also attached to the same heat sink. Theoretically, these two MOSFETs can handle up to 40A, 500V, which means that the total load dissipation can reach (20 kW). Practically, there are a number of limitations, like the power dissipated by the series resistance, and the heat transfer rate of the heat sink, but this can be solved by increasing the number of the MOSFETs. The used power MOSFET and its heat sink are shown in Figure 9.

This MOSFET is a voltage controlled current source using the circuit which is designed for this purpose. This circuit controls and senses the load current, which is equal the sum of currents of all MOSFETs, i.e. $(I_{total} = \sum_{n=1}^N i_n)$. It is mainly built using LM358N which has two rail-to-rail operational amplifiers. The implemented circuit worked satisfactorily. It also has connectors that drive the potentiometer and supply voltage for the fans, Arduino, and it links the control signals between the Arduino and the other peripherals. The circuit board is shown in Figure 10.

The system also includes:

- An external 12 V, 3 A power supply added to make it power standalone. It is obvious that it is not recommended to depend on the tested PV model power because it needs to be shorted during testing to measure the short circuit current.
- Two switches are used to control the 220 VAC, and the 12 VDC.
- An Arduino Mega 2560 to monitor the data, control current with software PID, read keypad, read the set point, and to transmit data to the computer at the serial port.
- A 10 A fuse is added in series with the PV load to protect the system from high current. The fuse rate must be less than $(N \times \min(i_{MOSFETmax}, i_{SensingMax}))$ where N is the number of parallel stages. In this design the MOSFET can handle up to 20 A, but the sensing resistor is rated at 5W, 0R1 ($I_{SensingMax} = \sqrt{P/R} = \sqrt{5/0.1} = 7.07 \text{ A}$). So, the fuse rate will be less than $[2 \times \min(20, 7.07)]$, that is less than $(2 \times 7.070 \text{ A})$.

Figure 11 shows different views of the practically implemented system.

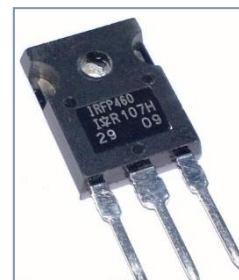


Fig. 9. The Power MOSFET and its Heat Sink

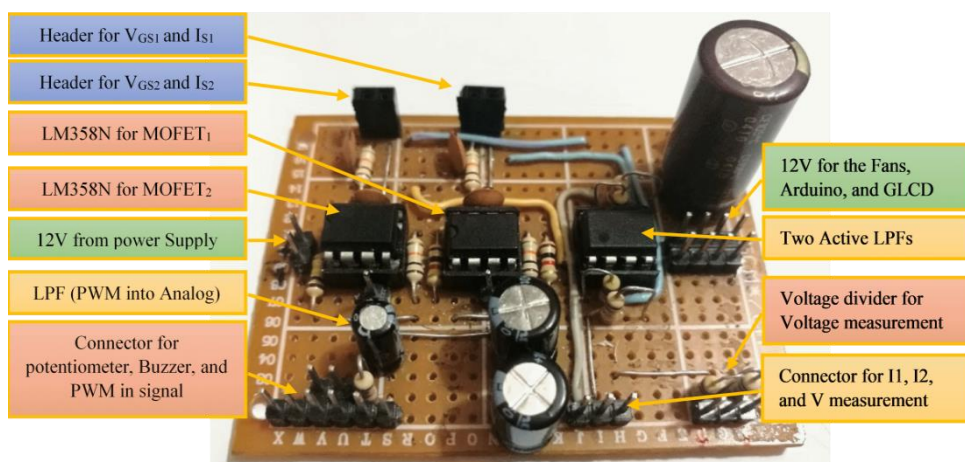


Fig. 10. The System Main Driving and Sensing Circuit Board

Results and Discussion

A PV panel was tested with the following manufacturing specifications ($V_{OC} = 24\text{ V}$, $I_{SC} = 0.5\text{ A}$). The system was connected to the solar panel as shown in Figure 12. Both modes were tested and they worked as expected. To discuss the results, the auto mode is selected. It starts by measuring the open circuit voltage V_{OC} before loading the panel. Then the system requests the panel current limitation I_{MAX} , it is optional because the system will stop increasing the current when the voltage drop to zero, but if the maximum current is set close to the I_{SC} , the reading will be more accurate. After that, the system starts by increasing the load in small-step of (0.01 A), until the voltage drops to zero, since the entered I_{MAX} is higher than the I_{SC} . The GLCD photo shows that the test is successful and it presented the designated data ($V_{MP} = 20.2\text{ V}$, $I_{MP} = 0.27\text{ A}$, $P_{MP} = 5.52\text{ W}$, $FF = 0.781$, $V_{OC} = 21.9\text{ V}$, and $I_{SC} = 0.32\text{ A}$).

All the measured data can be monitored and stored using the Arduino Serial monitor, or serial plotter. However, there is a software designed by Parallax, called

(PLX-DAQ) which has been used to read the data from the serial port and save them directly in the Microsoft Excel. This Excel file does not only give a report on the solar PV panel or array, but also can be used by researchers and students to analyze these data and detect any fault in the PV array. More data can be included in the report such; the sun location, and geolocation data based on astronomical calculations [21]–[24] and no adds on Figure 13 shows the test results of the mentioned PV panel and the I-V curve, P-V curve, and the PLX-DAQ window.

PV panel, string, or array can be tested by this device after connecting them directly to the device and faults can be detected based on the measured results and especially when the test performed on more than one panels connected in a serial or in a parallel array. Most faults occur in the blocking and bypass diodes as shown in Figure 14. Other faults may occur due to mismatching between the panels in the same string and that could happen for many reasons. Many faults signs can be recognized by this device, for example, a large drop in the string power may refer to ground fault, short circuit fault on one of the panels on the string, or most likely due to a mismatching effect of temporary or permanent reasons

[4]. The device is designed to measure and plot the P-V curve for the string to detect if there are many peak points which refer to a mismatching effect. Also, measuring a zero voltage on a single panel could indicate a short circuit in the bypass diode. Measuring no voltage on a string could refer to an open circuit in the blocking diode.

In a matter of the estimated system cost, Table 2 shows these estimated implementation costs from a specific supplier on a specific date. The overall cost (<160 USD) is cheap in comparison with other traditional system and the system capabilities.

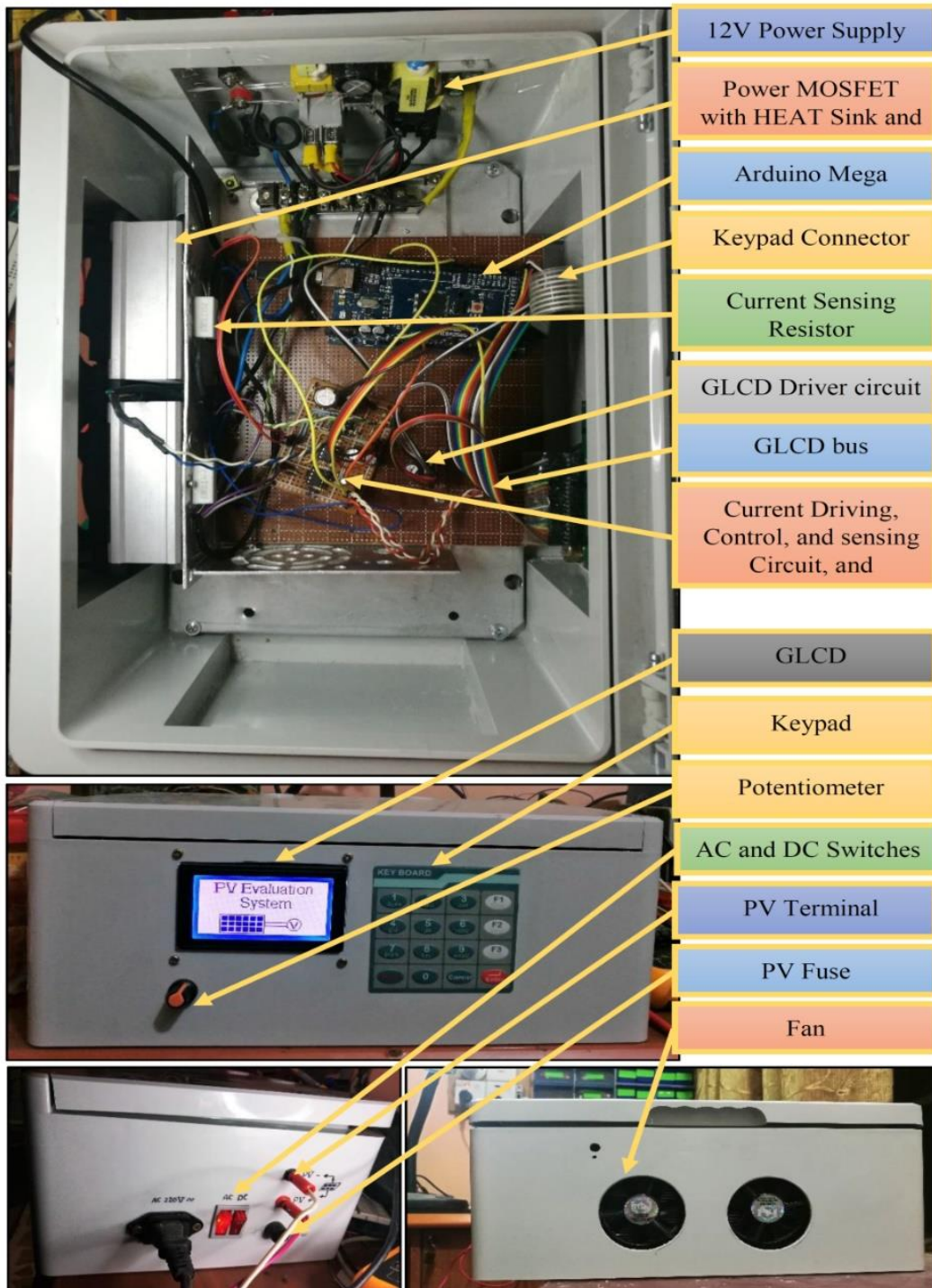


Fig. 11. The Implemented System

Table 2 Estimated Implementation Cost

Item No	Component	Specification	QTY	Total Cost (USD)
1.	Power MOSFET	IRFP460	1	\$3.95
2.	Heatsink with Fan		1	\$5.73
3.	Operation Amplifier	LM358N	2	\$1.04
4.	Power supply	12 V, 2 A.	1	\$14.74
5.	Microcontroller	Arduino Mega 2560	1	\$39.99
6.	GLCD	Optional	1	\$17.00
7.	Keypad	4x4	1	\$11.08
8.	Plastic Enclosure		1	\$16.78
9.	Series Resistor	0R1, 10 W	1	\$0.207
10.	Banana Power Jack		2	\$5.49
11.	Fuse with holder		1	\$3.62
12.	Resistors & Capacitors	Difference values	LS	\$10.0
13.	Rocker Switch	For AC and DC	2	\$4.36
14.	Mains Power Cord		1	\$4.41
15.	Power Entry Connector		1	\$2.58
16.	Potentiometer	50 kΩ		\$13.10
Total Cost				\$154.077*

* Prices are according to Farnell (<http://www.newark.com>) on Dec 12, 2018, and for +1, it is calculated for 20A maximum load, in case of the load increased there is more cost will add, every 20A added will add (Power MOSFET, heatsink with fan, and two operation amplifiers), the plastic Enclosure may need to be larger.

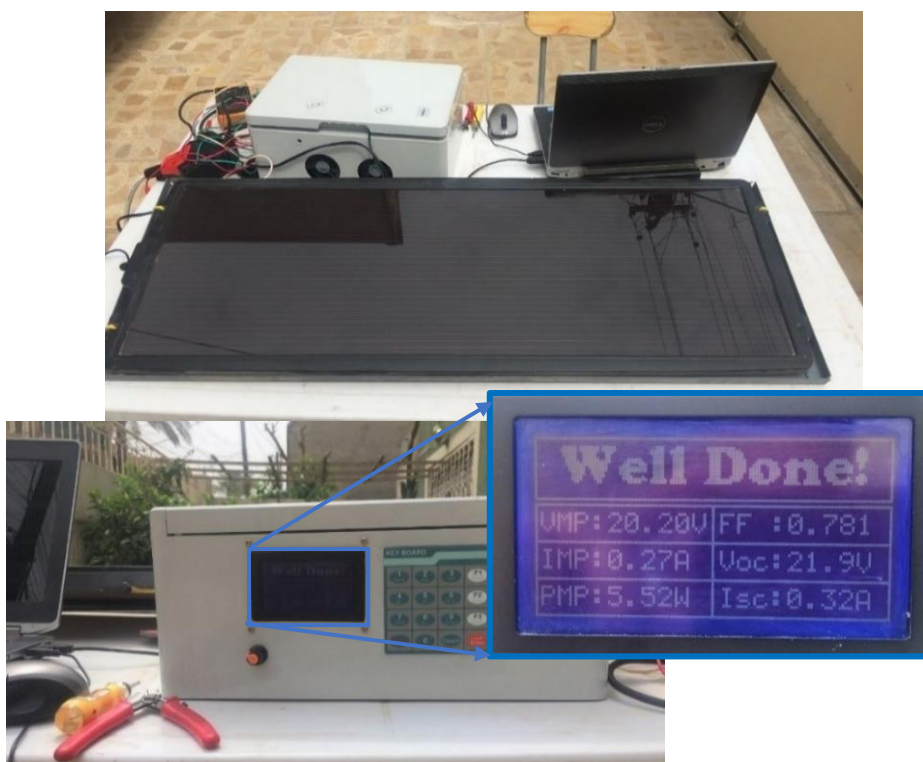


Fig. 12. A PV Panel under Test

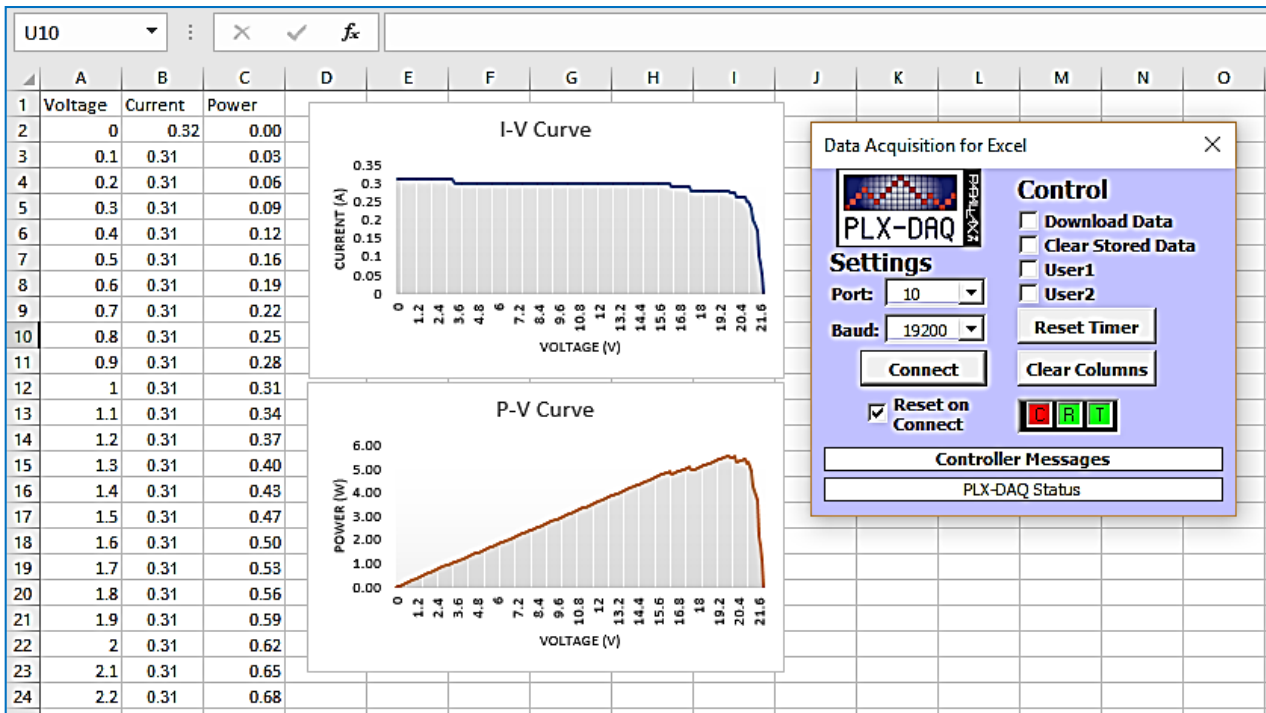


Fig. 13. An Automatically Generated Excel File

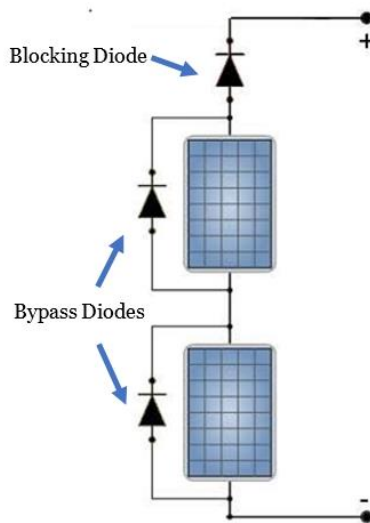


Fig. 14. PV String with the Blocking and Bypass Diodes

Conclusion

This article presents the design and implementation of low-cost electronic load and measurement system for on-site testing and evaluating the performance of the PV array. It collects data from the PV power plant by scanning the load and gives a clear vision for the power plant production, PV efficiency and fault detection. A Power N-channel MOSFET acts as an electronically controlled load that moves the PV panel operating point over the entire I-V characteristic curve, then displays and stores all the voltage, current, and power measurements. These data

will be used to produce a report that describes the PV power behavior in the field conditions. This report includes I-V characteristics curve, P-V characteristics curve, fill factor, the maximum power point and their corresponding voltage and current, open circuit voltage, and short circuit current. Design issues and mathematical models are described in an easy upgrading. Finally, the system has been practically implemented and worked satisfactory. Many design issues are solved to produce this final scheme.

References

- [1] Y. Kuai and S. Yuvarajan, "An electronic load for testing photovoltaic panels," *J. Power Sources*, vol. 154, no. 1, pp. 308–313, 2006. doi:[10.1016/j.jpowsour.2005.04.016](https://doi.org/10.1016/j.jpowsour.2005.04.016)
- [2] B. K. Bose, P. M. Szczesny, and R. L. Steigerwald, "Microcomputer Control of a Residential Photovoltaic Power Conditioning System," *IEEE Trans. Ind. Appl.*, vol. IA-21, no. 5, pp. 1182–1191, 1985. doi:[10.1109/TIA.1985.349522](https://doi.org/10.1109/TIA.1985.349522)
- [3] A. J. Abid, A. A. Obed, and F. M. Al-Naima, "Web-Based System Design to Monitor and Control the Mismatching Effects in a Vast Solar Farm," *Int. Energy J.*, vol. 18, no. 4, pp. 379 – 390, 2018.
- [4] A. Abid, A. Abid, A. Obed, and F. Al-Naima, "Detection and control of power loss due to soiling and faults in photovoltaic solar farms via wireless sensor network," *Int. J. Eng. Technol.*, vol. 7, no. 2, pp. 718–724, 2018.

- doi:[10.14419/ijet.v7i2.10987](https://doi.org/10.14419/ijet.v7i2.10987)
- [5] O. A. Al Ameri, M. A. Serhan, L. A. Lamont, and L. El Chaar, "Variable electronic load for testing PV performance," *Appl. Sol. Energy*, vol. 46, no. 2, pp. 89–96, 2010.
doi:[10.3103/S0003701X10020027](https://doi.org/10.3103/S0003701X10020027)
- [6] A. J. Abid, R. S. Ali, F. M. Al-Naima, Z. Ghassemlooy, and Z. Gao, "A new power line communication modem design with applications to vast solar farm management," *2013 3rd Int. Conf. Electr. Power Energy Convers. Syst. EPECS 2013*, vol. 4, no. 14, pp. 34–49, 2013.
doi:[10.1109/EPECS.2013.6713015](https://doi.org/10.1109/EPECS.2013.6713015)
- [7] U. Zimmermann and M. Edoff, "A maximum power point tracker for long-term logging of PV module performance," *IEEE J. Photovoltaics*, vol. 2, no. 1, pp. 47–55, 2012.
doi:[10.1109/JPHOTOV.2011.2174031](https://doi.org/10.1109/JPHOTOV.2011.2174031)
- [8] R. Patel, "Design and Implementation of an Isolated Solar Photovoltaic Power Generation System," National Institute of Technology, 2014.
- [9] K. Itoh, "Constant voltage power supply circuit and method of testing the same." Google Patents, Sep-2007.
- [10] T. S. Wurster and M. B. Schubert, "Mismatch loss in photovoltaic systems," *Sol. Energy*, vol. 105, pp. 505–511, 2014.
doi:[10.1016/j.solener.2014.04.014](https://doi.org/10.1016/j.solener.2014.04.014)
- [11] S. MacAlpine, C. Deline, R. Erickson, and M. Brandemuehl, "Module mismatch loss and recoverable power in unshaded PV installations," in *proceeding of the IEEE Photovoltaic Specialists Conference*, Austin, TX, USA, June 3-8 2012.
doi:[10.1109/pvsc.2012.6317858](https://doi.org/10.1109/pvsc.2012.6317858)
- [12] G. Makrides, B. Zinsser, M. Norton, and G. E., "Performance of Photovoltaics Under Actual Operating Conditions," in *Third Generation Photovoltaics*, 2012.
doi:[10.5772/27386](https://doi.org/10.5772/27386)
- [13] P. Manganiello, M. Balato, and M. Vitelli, "A Survey on Mismatching and Aging of PV Modules: The Closed Loop," *IEEE Trans. Ind. Electron.*, vol. 62, no. 11, pp. 7276–7286, 2015.
doi:[10.1109/tie.2015.2418731](https://doi.org/10.1109/tie.2015.2418731)
- [14] E. Díaz-Dorado, A. Suárez-García, C. Carrillo, and J. Cidrás, "Influence of the shadows in photovoltaic systems with different configurations of bypass diodes," in *proceeding of SPEEDAM 2010 - International Symposium on Power Electronics, Electrical Drives, Automation and Motion*, Pisa, Italy June 14-16, 2010.
doi:[10.1109/SPEEDAM.2010.5542226](https://doi.org/10.1109/SPEEDAM.2010.5542226)
- [15] G. W. Chang, Y. H. Chen, L. Y. Hsu, Y. Y. Chen, Y. R. Chang, and Y. D. Lee, "Study of impact on high PV-penetrated feeder voltage due to moving cloud shadows," in *proceeding of 2016 IEEE International Symposium on Computer, Consumer and Control, IS3C 2016*, Xi'an, China, July 4-6, 2016.
doi:[10.1109/IS3C.2016.269](https://doi.org/10.1109/IS3C.2016.269)
- [16] M. Mani and R. Pillai, "Impact of dust on solar photovoltaic (PV) performance: Research status, challenges and recommendations," *Renew. Sustain. Energy Rev.*, vol. 14, no. 9, pp. 3124–3131, 2010.
doi:[10.1016/j.rser.2010.07.065](https://doi.org/10.1016/j.rser.2010.07.065)
- [17] M. N. Akram and S. Lotfifard, "Modeling and Health Monitoring of DC Side of Photovoltaic Array," *IEEE Trans. Sustain. Energy*, vol. 6, no. 4, pp. 1245–1253, 2015.
doi:[10.1109/TSTE.2015.2425791](https://doi.org/10.1109/TSTE.2015.2425791)
- [18] A. R. Frey, D. G. Apt, and T. M. Tdi-dynaload, "Application note for New 500V Linear MOSFETs for a 120 kW Active Load," *Adv. Power Technol.*, 2000.
- [19] A. J. Abid, "Internet of Energy: A Design to Manage Energy Consumption for Off-Grid Building," *Int. J. Autom. Smart Technol.*, vol. 9, no. 1, pp. 13–22, 2019.
doi:[10.5875/ausmt.v9i1.1408](https://doi.org/10.5875/ausmt.v9i1.1408)
- [20] B. T. Donnellan, G. J. Roberts, P. A. Mawby, and A. T. Bryant, "Modelling of current sharing in paralleled current limiting superjunction MOSFETs with common gate drives," *Microelectron. Reliab.*, vol. 52, no. 3, pp. 497–502, 2012.
doi:[10.1016/j.microrel.2011.12.007](https://doi.org/10.1016/j.microrel.2011.12.007)
- [21] F. Al-Naima, R. Ali, and A. J. Abid, "Design of an Embedded Solar Tracking System Based on GPS and Astronomical Equations," *Int. J. Inf. Technol. Web Eng.*, vol. 9, no. 1, pp. 12–31, 2014.
doi:[10.4018/ijitwe.2014010102](https://doi.org/10.4018/ijitwe.2014010102)
- [22] F. M. Al-Naima, R. S. Ali, and A. J. Abid, "Design and Implementation of a Smart Dual Axis Sun Tracker Based on Astronomical Equations," in *EWRES - The European Workshop on Renewable Energy Systems*, 2012.
- [23] F. M. Al-Naima, R. S. Ali, and A. J. Abid, "Design of a Control and Data Acquisition System for a Multi-Mode Solar Tracking Farm," in *EWRES - The European Workshop on Renewable Energy Systems*, 2012.
- [24] A. J. Abid, "Arduino Based Blind Solar Tracking Controller," *An Int. Open Access Journal, IETI Trans. Comput.*, vol. 5, no. 10, pp. 24–29, 2017.

 ©The Authors. This work is licensed under the Creative Commons Attribution-NonCommercial-NoDerivatives 4.0 International License.